Locomotion control of *Caenorhabditis elegans* through confinement – Supplementary Information –

Félix Lebois[1], Pascal Sauvage[1], Charlotte Py[1], Olivier Cardoso[1], Benoît Ladoux[1,2], Pascal Hersen[1,2], Jean-Marc Di Meglio[1*]

[1]Matière et Systèmes Complexes
UMR 7057 CNRS and University Paris Diderot
75013 Paris, France

[2]Mechanobiology Institute, Singapore
National University of Singapore
T-Lab, 5A Engineering Drive 1
Singapore, 117411

[*]Correspondence: jean-marc.dimeglio@univ-paris-diderot.fr

1 Data statistics

Phenotype variability of WT worms

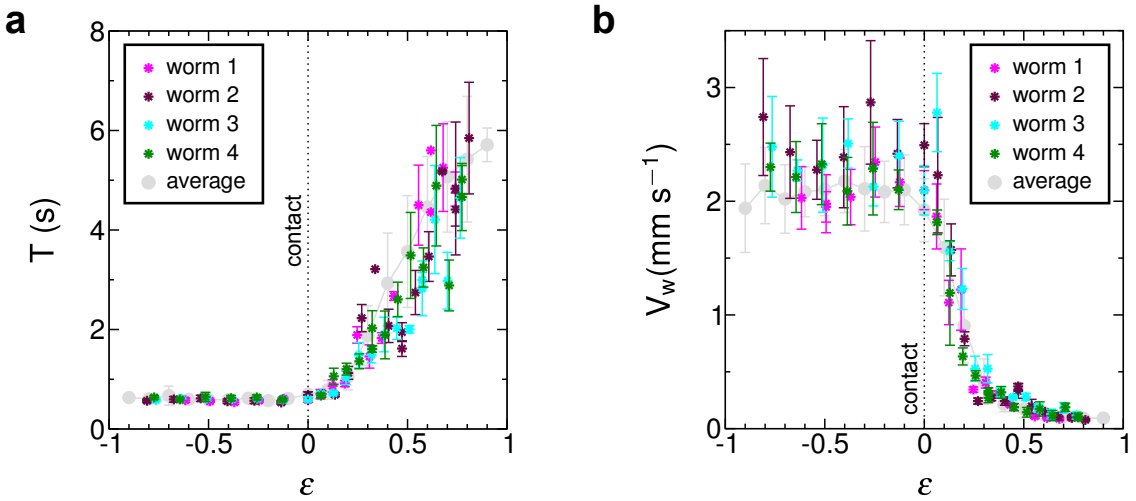

FIGURE S1 Evolution of kinematic parameters with confinement : statistics. Measurements for four individual wild type (WT) worms (worm 1, worm 2, worm 3, worm 4) compared to the average over 12 WT worms (in grey). Each colour point represents, for a single animal and for a determined confinement parameter ϵ, the average of several measurements (depending on the confinement, about 15 in average) on the worm trajectory. (a) period T. (b) wave propagation velocity V_w. In both graphs, error bars on average data (grey points) represent the standard deviation over the 12 worms, while error bars on individual data (colour points) represent the standard deviation for the data collected from a single worm trajectory.

Phenotype discrimination between WT and mutants

T	$\epsilon = -0.5$	$\epsilon = -0.3$	$\epsilon = 0.5$	$\epsilon = 0.7$
unc-79	0.003 (>)	0.003 (>)	0.332	0.794
trp-4	0.213	0.917	0.023 (<)	0.000 (<)
mec-4	0.435	0.055	0.627	0.102

V_w	$\epsilon = -0.5$	$\epsilon = -0.3$	$\epsilon = 0.5$	$\epsilon = 0.7$
unc-79	0.000 (<)	0.000 (<)	0.360	0.069
trp-4	0.875	0.818	0.005 (>)	0.000 (>)
mec-4	0.000 (>)	0.008 (>)	0.288	0.063

TABLE S1 Comparison of the period T and the wave propagation velocity V_w of mutants versus wild type for several values of the confinement parameter ϵ: p-values calculated according to the Kolmogorov-Smirnov test. In the cases where the two distributions are found significantly different ($p < 0.05$), we indicate whether the period/velocity of the mutant is higher (>) or smaller (<) than the wild type.

2 Backward locomotion

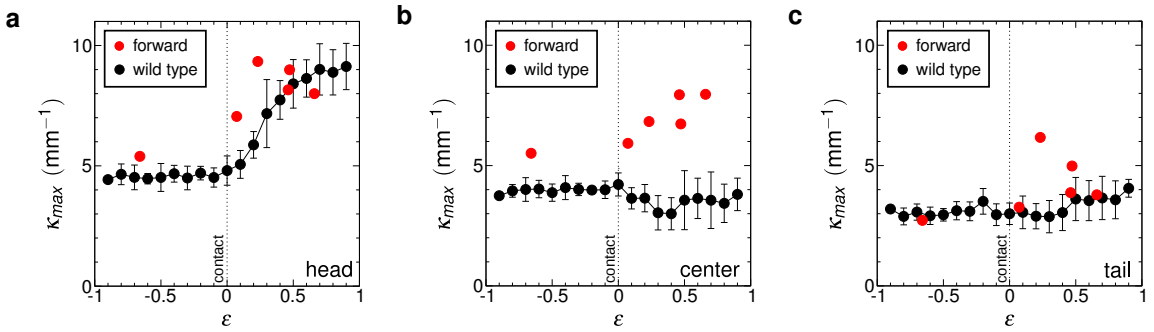

FIGURE S2 Backward locomotion (triangles) *vs* forward locomotion (circles) of WT worms: maximal curvature of the body at the head (left), center (middle) and tail (right).

3 Effect of confinement on the worm hydrodynamics

Microorganisms swim faster close to a solid boundary. This has been modelled in great details by Katz (1). In this section we present simpler physical arguments to explain the velocity increase in the swimming regime as ϵ approaches zero (Fig. 2c). We model the physical situation in Fig. S3.

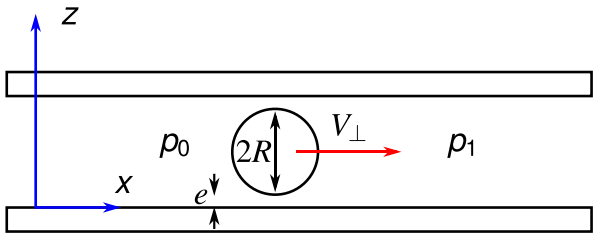

FIGURE S3 Hydrodynamics of a swimming worm. The problem is reduced to 2D. The worm (circular cross-section of radius R) is confined between two walls in a liquid of thickness $2(R+e)$. The transverse velocity of the worm is $V_\perp$. p_1 and p_0 respectively are the upstream pressure and the downstream pressure.

The flow profile $v_x(x,z)$ is ruled by the Stokes equation:

$$\eta \nabla_z^2 v_x(x,z) = \nabla_x p(x) \tag{1}$$

with η the liquid viscosity and p the pressure. We use of the lubrication approximation since most of the dissipative processes take place in the thin gap between the cylinder and the walls. From Eq. 1, using usual no-slip conditions at interfaces, we obtain:

$$v_x(z) = \frac{\nabla_x p(x)}{2\eta}(z^2 - h(x)z) + V_\perp \frac{z}{h(x)} \tag{2}$$

with $h(x)$ the distance between the plane and the cylinder ($h(0) = e$). The corresponding liquid flow (per unit length) $Q(x)$ is given by :

$$Q(x) = 2\int_0^{h(x)} v_x(z) = -\frac{\nabla_x p(x)}{\eta}\frac{h(x)^3}{6} + V_\perp h(x) \tag{3}$$

and remains constant along x and equal to $-2RV_\perp$ (*ie* the volume of liquid (per unit time and unit length) transferred from right to left, cf. Fig. S5). The pressure gradient then reads:

$$\nabla_x p(x) = 6\eta V_\perp \frac{2R + h(x)}{h^3(x)} \tag{4}$$

We can approximate the pressure difference $p_1 - p_0$ by:

$$p_1 - p_0 = 2\sqrt{Re}\nabla_x p(0) = 24\eta V_\perp \sqrt{Re}\frac{R + (1/2)e}{e^3} \simeq \frac{24\eta V_\perp}{R}(-\epsilon)^{-5/2} \tag{5}$$

where we have used the confinement parameter $\epsilon = -e/R$, assumed that $-\epsilon \ll 1$ (*ie* for situations of near confinements) and introduced the characteristic horizontal length scale of the problem $\sqrt{Re}$. The associated force (per unit length) is :

$$F_\perp = 48\eta V_\perp (-\epsilon)^{-5/2} \tag{6}$$

There is another contribution to $F_\perp$ due to viscous stresses:

$$2\eta\frac{V_\perp}{e}2\sqrt{Re} = 4\eta V_\perp(-\epsilon)^{1/2} \sim (-\epsilon)^{-1/2} \tag{7}$$

which is negligible with respect to the pressure component (Eq. 6) when $-\epsilon \to 0$. The longitudinal viscous force (per unit length) $F_\parallel$ is given by:

$$F_\parallel = 2\eta\frac{V_\parallel}{e}2\sqrt{Re} = 4\eta V_\parallel(-\epsilon)^{-1/2} \tag{8}$$

We finally eventually obtain the ratio of the friction coefficients (per unit length) $c_\perp$ and $c_\parallel$ (defined by $F_{\perp,\parallel} = c_{\perp,\parallel}V_{\perp,\parallel}$):

$$c_\perp/c_\parallel = 12(-\epsilon)^{-2} \tag{9}$$

This ratio diverges as $-\epsilon \to 0$, as observed in recent experiments (2). The estimated ratio can now be used to predict the velocity V of the worm. We use the expression established by Gray and Lissmann (3)(for a review of nematode locomotion, see (4)) which states:

$$V = V_w\,\frac{(c_\perp/c_\parallel) - 1}{(c_\perp/c_\parallel) + 2(Aq)^{-2}} \tag{10}$$

where $V_w = 2\pi/(qT)$. q is the wave number of the undulation, T its period and A its amplitude. Eq. 10 is valid for small amplitudes (i.e. for $Aq < 1$). $Aq \simeq 0.5\pi$ for swimming *C. elegans* (and then $2(Aq)^{-2} \simeq 1$) and we have then by extrapolation of the validity domain of Eq. 10 ($\epsilon < 0$):

$$V \simeq V_w\frac{12 - \epsilon^2}{12 + \epsilon^2} \tag{11}$$

This prediction is not sophisticated enough to be compared with actual experiments but it contains all necessary physical ingredients and understands that the worm velocity should increase as the gap between the confining walls approaches the worm diameter, as it is indeed observed.

4 Worms crawling on agar gels

The motion of wild type (WT) *C. elegans* as well as of mutant strains *trp-4(sy695)*, *mec-4(e1611)* and *unc-79(e1068)* was recorded while the worms moved forward on plane agar gels, for the sake of comparison with the locomotion in confined conditions. Worms were washed in M9 buffer and then transferred to an agar plate (2 % agar) without food. Parameters of the locomotion such as the period T, the wave velocity along the body V_w, the maximal curvature along the body κ_{max} and the displacement velocity V were measured as described above. Results, as well as projections of the worm midline over time, are shown on Fig. S6.

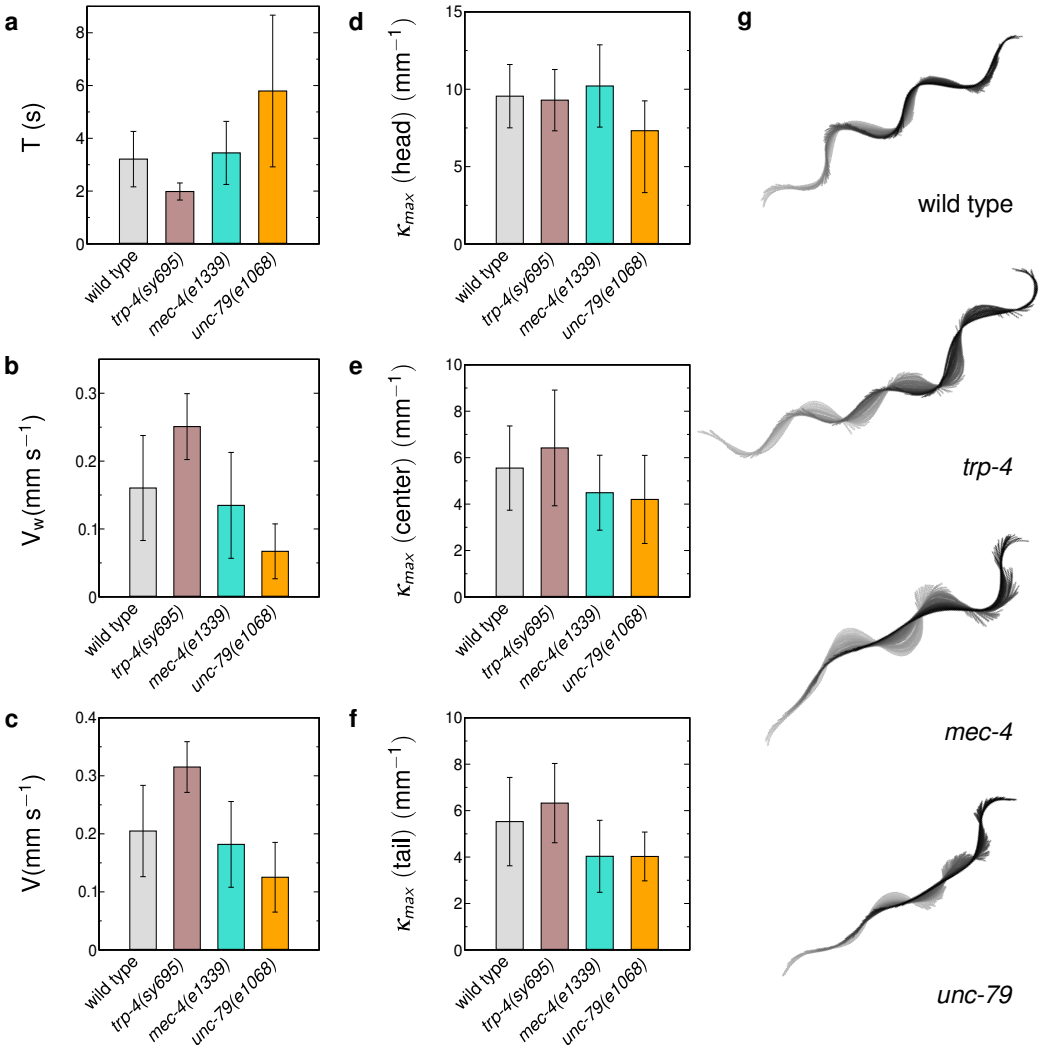

FIGURE S4 *C. elegans* locomotion on agar gel. (a) period. (b) wave propagation velocity. (c) worm velocity. (d) maximal curvature at the head ($s = 0.1$). (e) maximal curvature at the center of the body ($s = 0.5$). (f) maximal curvature at the tail ($s = 0.9$). (g) projections of the worm midline over approximatively 2 periods of the movement, for (from top to bottom): wild type, *trp-4(sy695)*, *mec-4(e1611)*, *unc-79(e1068)*. The presented values are average values over about ten worms for each mutant. Error bars indicate standard deviation.

5 Principal Component Analysis and eigenworms

For each value of ϵ we computed the first four *eigenworms*, using Principal Component Analysis as described by Stephens *et al.* (5). For each video frame, the worm midline is described by a set of $N+1$ points x_i evenly distributed along the body that allow to compute the N angles φ_i between the tangent vector to the body midline at x_i and the horizontal direction (Fig. S7). The image is rotated so that the average of the angles along the body is zero:

$$\frac{1}{N}\sum_{i=1}^{N}\varphi_i = 0. \tag{12}$$

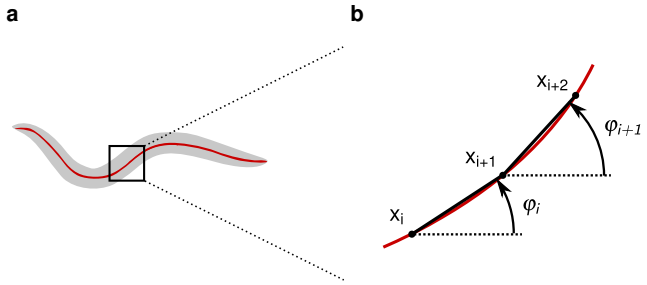

FIGURE S5 Worm body parametrisation. (a) the shape of the worm is reduced to the body midline using a smoothing spline, as described in Methods. (b) the N angles φ_i are defined as the tangent vector to the body midline at x_i and the horizontal direction.

$\varphi_i(t)$ thus provides a complete description of the worm shape over time in its own frame, as an alternative to the local curvature $\kappa_i(t)$. The covariance matrix of the angles is:

$$C_{ij} = \langle(\varphi_i - \langle\varphi_i\rangle)(\varphi_j - \langle\varphi_j\rangle)\rangle, \tag{13}$$

where $\langle\rangle$ indicates the average over the successive shapes adopted by the worm. Eigenvalues λ_μ and eigenvectors $\mathbf{u}_\mu$ (also called *eigenworms*) of the covariance matrix are computed and indexed in order of decreasing eigenvalues, from all the movies corresponding to the given ϵ. In contrast with Stephens *et al.* we only consider video frames where the worm crawls forward. For all values of the confinement parameter, we found that the first four eigenworms account for more than 99 % of the total variance. Therefore we do not use the eigenvectors $\mathbf{u}_\mu$ with $\mu > 4$ to compute the shapes presented in Fig. 2e. Examples of the first four eigenvectors for three values of the confinement parameter ($\epsilon = -0.5$, $\epsilon = 0$, $\epsilon = 0.5$) are given in Fig. S8. We define the average worm for a given ϵ as the average of these first four *eigenworms* weighted by the square root of the corresponding eigenvalues:

$$\mathbf{w} = \sum_{\mu=1}^{4}\sqrt{\lambda_\mu}\mathbf{u}_\mu. \tag{14}$$

The shapes presented in Fig. 2e are reconstructed from the angles vector $\mathbf{w}$. This approach is meaningful as long as the trajectory followed by the worm in the space of shapes $(\varphi_i)_{1\leq i\leq N}$ is periodical. Besides, the information concerning the phase shift of the oscillation of the

coordinates in the principal component space is lost. Thus the shapes of Fig. 2e should not be considered as real shapes, but rather as fictitious shapes capturing the essential features of the worm body postures for a given ϵ.

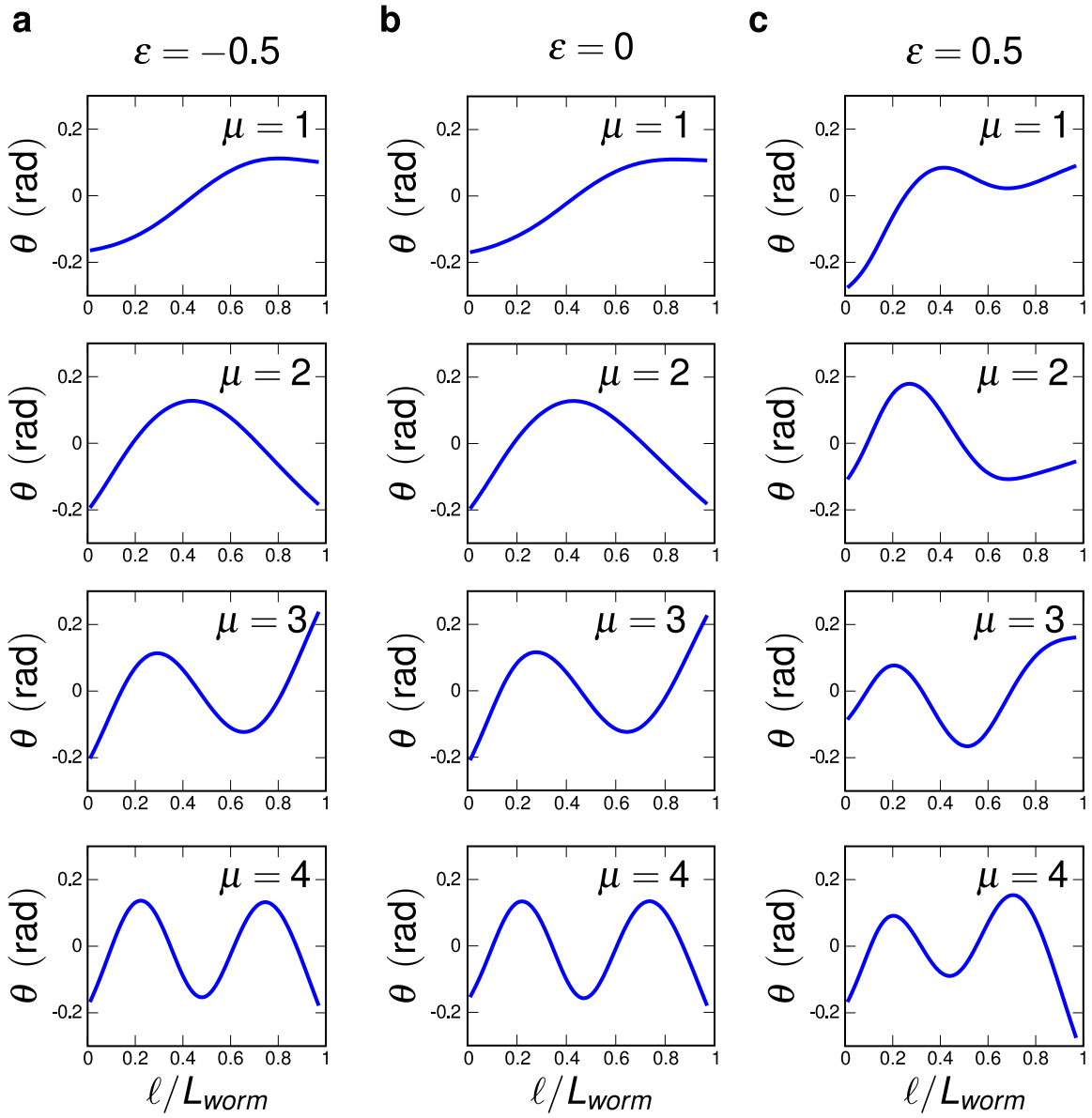

FIGURE S6 Eigenworms. The first four principal components, for three values of ϵ: (a) $\epsilon = -0.5$; (b) $\epsilon = 0$; (c) $\epsilon = 0.5$.

6 Continuous compression of WT worms

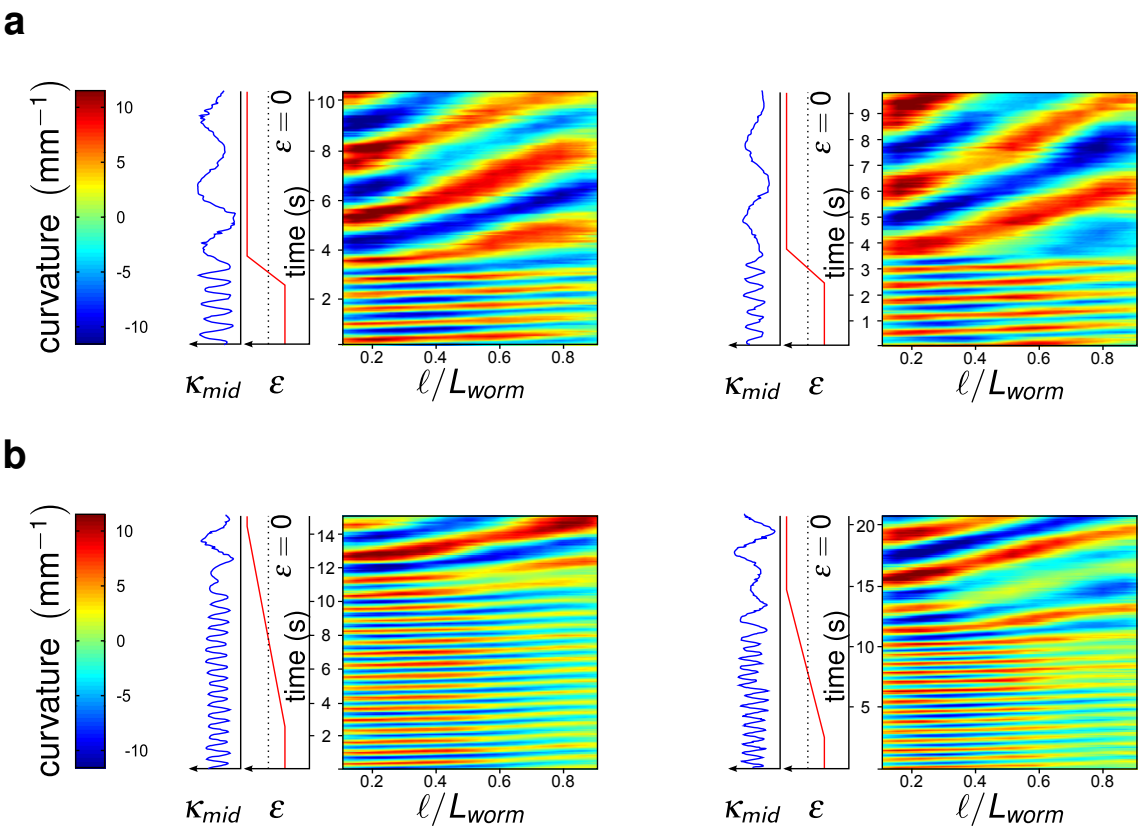

FIGURE S7 Examples of progressive compression of a WT worm. Upper graphs, fast compression $\left(\frac{d\epsilon}{dt} = -0.7\,\mathrm{s}^{-1}\right)$; lower graphs, slow compression $\left(\frac{d\epsilon}{dt} = -0.07\,\mathrm{s}^{-1}\right)$ (see Fig. 1 for curvature color scale). As for continuous release experiments, the worm instantaneously adapts its locomotion pattern.

Supporting references

1. Katz, D., 1974. On the propulsion of micro-organisms near solid boundaries. *Journal of Fluid Mechanics* 64:33–49.

2. Semin, B., J. P. Hulin, and H. Auradou, 2009. Influence of flow confinement on the drag force on a static cylinder. *Physics of Fluids* 21:103604.

3. Gray, J., and H. Lissmann, 1964. The locomotion of nematodes. *Journal of Experimental Biology* 41:135–154.

4. Alexander, R., 2002. Locomotion. *In* D. Lee, editor, The Biology of Nematodes, Taylor and Francis Inc.

5. Stephens, G. J., B. Johnson-Kerner, W. Bialek, and W. S. Ryu, 2008. Dimensionality and Dynamics in the Behavior of C. elegans. *PLoS Computational Biology* 4:e1000028.